LPV Model-Based Multivariable Indirect Adaptive Control of Damaged Asymmetric Aircraft

Jing Zhang[1]; Xieyu Xu[2]; Lingyu Yang[3]; and Xiaoke Yang[4]

Abstract: Owing to the complexity of aircraft structural damage, directly measuring the pattern and severity of damage using onboard sensors is difficult. This paper proposes a linear parameter-varying (LPV) model–based online estimation and indirect adaptive control scheme for aircraft with severe structural damage. Specifically, the unmeasurable damage parameters are designed as the gain scheduling coefficients (GSCs) of the LPV model. By employing the proposed LPV model, the online computational load is significantly reduced compared with that of typical existing methods. Furthermore, an online identification algorithm with a Lyapunov stability guarantee is presented to estimate the GSCs, and an online-designed model reference controller that combines a state-feedback decoupling controller and a disturbance rejection term is adopted to implement attitude control. The closed-loop system is simulated with the National Aeronautics and Space Administration (NASA) generic transport model under a left wing tip damage scenario. The simulation results demonstrate that the proposed method can estimate GSCs and the uncertainty of the aircraft rapidly and accurately, and the closed-loop system precisely achieves the desired attitude responses. **DOI: 10.1061/(ASCE)AS.1943-5525.0001089.** © *2019 American Society of Civil Engineers.*

Introduction

Modern aircraft, despite their advanced instrumentation and various fault-tolerant designs, are still susceptible to unexpected conditions, e.g., turbulence, wind gusts, structural fatigue, bird strikes, and aging, which may cause damage to the aircraft's structure (Bacon and Gregory 2007; Airplanes, Boeing Commercial 2016). Abrupt structural damage may lead to significant changes in an aircraft's aerodynamics, mass properties, symmetry, and so forth, posing challenges for both handling quality and flight safety (Kim et al. 2014; Wang et al. 2016; Pei et al. 2016). Although many new sensing techniques focus on this problem (Di Sante 2015; Qiu et al. 2016), directly measuring all the patterns and severities of the damage patterns and the severities using onboard sensors remains difficult. Indirect approaches, such as online identification and adaptive control, which are based on changes in an the aircraft's dynamics, are gradually increasing in popularity.

Nguyen et al. (2008) proposed an artificial neural network (ANN)–based hybrid adaptive control scheme to maintain the stability and command tracking performance of a damaged aircraft. A pretrained ANN-based adaptive estimation block was used to generate the dynamic inversion of damaged aircraft, and another online learning ANN was designed as a compensator. Bao et al. (2011) used a radial basis function neural network to detect and isolate wing structural damage. Chowdhary et al. (2013) adopted a single-layer ANN to approximate the model error, which serves as an adaptive pseudo-input for an existing dynamic inversion controller. This method was successfully validated through experimentation on a fixed-wing unmanned aerial system under actuator failures and some severe structural damage scenarios. In addition to indirect neural network adaptive control algorithms, direct approaches have also received significant attention (Tao 2014). Stepanyan et al. (2010) introduced a modified model reference adaptive control method, in which roll rate, pitch rate, and sideslip angle controllers were designed separately. Liu et al. (2010) and Guo et al. (2011) treated aircraft as a multiple-input, multiple-output (MIMO) system and proposed a multivariate model reference adaptive control (MMRAC) scheme. A state-feedback controller was employed under a model matching condition. Linearization of the nonlinear dynamics of damaged aircraft into a piecewise linear system was also conducted and analyzed to facilitate controller design. Guo and Tao (2012, 2015) and Guo et al. (2014) further developed a discrete-time form of the MMRAC scheme and validated the development using the National Aeronautics and Space Administration (NASA) generic transport model (GTM) with left wing tip loss.

A significant problem when applying an adaptive control algorithm to a MIMO system, such as a damaged aircraft, is the large number of estimated parameters. The adaptive law needs to estimate parameter matrices rather than a few scalar variables; for example, in Nguyen et al. (2008), the indirect adaptive law estimates three matrices online to compensate for model error, and in Guo et al. (2011, 2014) and Guo and Tao (2012), the parameters to be estimated consist of a state feedback matrix, an input matrix, and a disturbance compensation vector. The large number of parameters increases the computational complexity and the difficulty in designing the adaptation gains. Meanwhile, prior knowledge can effectively reduce the complexity of an adaptive controller, such as a pretrained ANN (Nguyen et al. 2008; Chowdhary et al. 2013) and offline analysis, where in wing-level flight conditions, signs of leading principal minors of the high-frequency gain matrix are known and invariant under damage (Guo et al. 2011; Guo and Tao 2015).

[1]Assistant Professor, School of Automation Science and Electrical Engineering, Beihang Univ., Beijing 100191, China. ORCID: https://orcid.org/0000-0002-5217-8439. Email: Zhangjing2013@buaa.edu.cn

[2]Research Assistant, Dept. of Control Technology, CNIGC Institution of Navigation and Control, Beijing 100089, China. Email: xudavid501@163.com

[3]Associate Professor, School of Automation Science and Electrical Engineering, Beihang Univ., Beijing 100191, China (corresponding author). Email: yanglingyu@buaa.edu.cn

[4]Postdoctor, School of Automation Science and Electrical Engineering, Beihang Univ., Beijing 100191, China. ORCID: https://orcid.org/0000-0002-9029-4545. Email: xiaokeyang@buaa.edu.cn

Note. This manuscript was submitted on September 7, 2017; approved on June 4, 2019; published online on August 20, 2019. Discussion period open until January 20, 2020; separate discussions must be submitted for individual papers. This paper is part of the ***Journal of Aerospace Engineering***, © ASCE, ISSN 0893-1321.

Thus, taking advantage of the a priori knowledge to reduce the number of adaptive parameters is a key issue for multivariable adaptive control. From this observation and inspired by the methods in Guo et al. (2011) and Guo and Tao (2012), this paper proposes a LPV model–based multivariable indirect adaptive control (LPVM-MIAC) scheme that includes three parts: offline LPV modeling, online identification of gain scheduling coefficients (GSCs) and the uncertainty term, and online design of the decoupling controller. The main contributions of this paper are as follows. (1) To address the large number of adaptive parameters that accompany the MIMO system and various damage conditions of aircraft, a moderate-size polytopic LPV modeling technique is developed for aircraft in various damage conditions. This technique consists of the a priori analysis of aircraft damage conditions and a model reduction approach, distributing some of the online computations to the offline design process. This LPV model effectively reduces the online-identified parameters to only a few GSCs and an uncertainty term. (2) An LPVM-MIAC scheme is developed to solve the online identification and controller design problem for the resulting LPV model. In particular, an online constrained identification algorithm for the GSCs and uncertainty of the LPV model is proposed. Note that the difference between this method and the LPV model identification (Giani et al. 2012) or LPV observer-based fault control approach (Zhang et al. 2016; Jia et al. 2014) is that the last two assume that GSCs are measurable and are used to estimate the system states or parameters. In contrast, the proposed method focuses on the online GSC identification problem. The identified LPV model then fits into a standard model reference controller, which combines a state-feedback decoupling controller and a disturbance rejection block for offset-free output tracking with desired closed-loop dynamics.

The remainder of this paper is organized as follows. The second section presents the LPV modeling of structurally damaged aircraft. The third section discusses the identification of the GSCs and the LPV model. Then the design of the model reference controller is presented in detail. A case study on the NASA GTM with a left wing tip loss scenario is performed in the fourth section, and the simulation results are analyzed therein. The fifth section then summarizes the method and proposes future research directions.

LPV Modeling of Structurally Damaged Aircraft

Piecewise Linear Models

The GTM developed by NASA Langley Research Center is used for this study. It is a notional twin-engine transport-class aircraft that can support simulations of various types of structural damage scenarios. The modeling of the nonlinear dynamics of the GTM was thoroughly studied by Bacon and Gregory (2007), Nguyen et al. (2008), and Bailey et al. (2005), and it can be described by the following general nonlinear ordinary differential equation (ODE) form:

$$\dot{\boldsymbol{x}} = \boldsymbol{f}(\boldsymbol{x}, \boldsymbol{u}, \boldsymbol{\lambda}) \tag{1}$$

where $\boldsymbol{x} = [\nu, \alpha, q, \theta, \beta, p, r, \phi]^\top \in \mathbb{R}^n$ is the state vector. The elements in x represent airspeed (m/s), angle of attack (degrees), pitch rate (degrees/s), pitch angle (degrees), sideslip angle (degrees), roll rate (degrees/s), yaw rate (degrees/s), and roll angle (degrees), respectively. $\boldsymbol{u} = [u_e, u_a, u_r]^\top \in \mathbb{R}^m$ is the input vector, which includes the deflection (degrees) of the elevator, the aileron, and the rudder. A parameter vector $\boldsymbol{\lambda} \in \mathbb{R}^v$ is used to represent the severity of v types of damage, such as wing tip off, vertical tail off, and left stabilizer off. In particular, $\boldsymbol{\lambda}$ is unmeasurable and is assumed to be in a known convex set, such as

$$\boldsymbol{\lambda} \in \boldsymbol{\Omega}_{\boldsymbol{\lambda}} \triangleq \{\lambda_i | 0 \le \lambda_i \le \lambda_{i_{\max}} \le 1, i = 1, \ldots, v\} \tag{2}$$

where $\lambda_{i_{\max}}$ represents the maximum damage severity of the ith damage scenario covered by the model. Note that in some very serious damage situations, the aircraft cannot be saved even if there is a perfect controller; thus, $\lambda_{i_{\max}}$ is used to exclude the unrecoverable damage scenarios. In the present case, based on the offline analysis results, $\boldsymbol{\lambda} \in \boldsymbol{\Omega}_{\boldsymbol{\lambda}}$ is set such that the aircraft can be trimmed within the actuator constraints. Assume that the aircraft is operating in the linear zone of the aerodynamics, i.e., in a small angle of attack; then Eq. (1) can be linearized around an operating point $(\boldsymbol{x}_0, \boldsymbol{u}_0)$, leading to a perturbed representation

$$\Delta\dot{\boldsymbol{x}} = \boldsymbol{A}(\boldsymbol{\lambda})\Delta\boldsymbol{x} + \boldsymbol{B}(\boldsymbol{\lambda})\Delta\boldsymbol{u} + \boldsymbol{f}_0(\boldsymbol{\lambda}) + \boldsymbol{O} \tag{3}$$

where

$$\Delta\boldsymbol{x} = \boldsymbol{x} - \boldsymbol{x}_0, \quad \Delta\boldsymbol{u} = \boldsymbol{u} - \boldsymbol{u}_0$$
$$\boldsymbol{A}(\boldsymbol{\lambda}) = \partial\boldsymbol{f}(\boldsymbol{x}, \boldsymbol{u}, \boldsymbol{\lambda})/\partial\boldsymbol{x}|_{(\boldsymbol{x}_0, \boldsymbol{u}_0)}, \quad \boldsymbol{B}(\boldsymbol{\lambda}) = \partial\boldsymbol{f}(\boldsymbol{x}, \boldsymbol{u}, \boldsymbol{\lambda})/\partial\boldsymbol{u}|_{(\boldsymbol{x}_0, \boldsymbol{u}_0)}$$

The affine term $\boldsymbol{f}_0(\boldsymbol{\lambda}) = \boldsymbol{f}(\boldsymbol{x}_0, \boldsymbol{u}_0, \boldsymbol{\lambda})$ represents disturbances caused by the damage and may not be 0. $\boldsymbol{O}$ denotes higher-order terms.

Note that $\boldsymbol{A}$, $\boldsymbol{B}$, and $\boldsymbol{f}_0$ are functions of $\boldsymbol{\lambda}$, and an approximation for Eq. (3) is to grid the parameter space $\Omega_{\boldsymbol{\lambda}}$. Suppose that there are v types of damage and that the jth $\in \{1, \ldots, v\}$ damage scenario can be divided into k_j levels based on severity; then one can compute a local linear model at each grid point $\boldsymbol{\lambda}_{i_1, i_2, \ldots, i_v}$, where $i_j = (1, \ldots, k_j)$ is the grid index for the jth damage scenario. For convenience, this paper uses the notation # to represent the grid index $i_1, i_2, \ldots, i_v$ in the following derivation. Thus, a piecewise linear model is given by

$$\Delta\dot{\boldsymbol{x}} = \sum_{i_1=1}^{k_1}\sum_{i_2=1}^{k_2}\cdots\sum_{i_v=1}^{k_v}\left[\prod_{j=1}^{v}\omega_{j,i_j}(\boldsymbol{\lambda})\right][\boldsymbol{A}_{\#}\Delta\boldsymbol{x} + \boldsymbol{B}_{\#}\Delta\boldsymbol{u} + \boldsymbol{f}_{0_{\#}}] \tag{4}$$

where $[\boldsymbol{A}_{\#}, \boldsymbol{B}_{\#}, \boldsymbol{f}_{0_{\#}}]$ is the linear time-invariant local model at each grid point. The weighting function $\omega_{j,i_j}(\boldsymbol{\lambda})$:$\mathbb{R}^v \mapsto \mathbb{R}$ satisfies the following relations:

$$\omega_{j,i_j}(\boldsymbol{\lambda}) \in \{0, 1\}$$
$$\sum_{i_j=1}^{k_j}\omega_{j,i_j}(\boldsymbol{\lambda}) = 1, \quad (j = 1, \ldots, v \quad \text{and} \quad i_j = 1, \ldots, k_j) \tag{5}$$

Polytopic LPV Models

There are two typical approaches to using Eq. (4) in damaged aircraft flight control. The first is to treat the weighting functions as unknown and use the idea of the multiple-model adaptive estimation (MMAE) method (Lu et al. 2015; Jung et al. 2009). This method uses a parallel bank of filters to provide multiple estimates, and each filter corresponds to a possible damage condition, i.e., a local model. The weighting functions $\omega_{j,i_j}(\boldsymbol{\lambda})$ are calculated by the likelihood function of each filter. The accuracy of the estimation then depends on the fineness of the grid. A significant computational load may be introduced when using a fine grid. The other method is to treat all the local models as unknown in the adaptive control law design process (Guo et al. 2011); then the parameters to be determined or estimated depend on the size of $[\boldsymbol{A}_{\#}, \boldsymbol{B}_{\#}, \boldsymbol{f}_{0_{\#}}] \in \mathbb{R}^{n\times(n+m+1)}$, which could be very large in practice.

To address this problem of the piecewise model, the higher-order singular value decomposition (HOSVD) method in Baranyi 2016)) and Sun et al. (2016) is used to reduce the number of local models without losing much accuracy. Set

$$S_{\#} = [A_{\#}, \quad B_{\#}, \quad f_{0_{\#}}] \tag{6}$$

and stack all the $S_{\#}$ to create a model tensor $\mathcal{S} \in \mathbb{R}^{k_1 \times k_2 \times \ldots \times k_v \times n \times (n+m+1)}$; then Eq. (4) can be rewritten in tensor product (TP) form (Baranyi 2016) as

$$\Delta \dot{\boldsymbol{x}} = \mathcal{S} \boxtimes_{j=1}^{v} \boldsymbol{\Omega}_j \begin{bmatrix} \Delta \boldsymbol{x} \\ \Delta \boldsymbol{u} \\ 1 \end{bmatrix} \tag{7}$$

where the column vector $\boldsymbol{\Omega}_j = [\omega_{j,1}, \omega_{j,2}, \ldots \omega_{j,k_j}]^{\top}$. Using the HOSVD technique, the TP term $\mathcal{S} \boxtimes_{i=1}^{v} \boldsymbol{\Omega}_i$ can be reduced by omitting the small singular values. With this algorithm, the full TP model can be approximated as

$$\mathcal{S} \boxtimes_{j=1}^{v} \boldsymbol{\Omega}_j \approx \mathcal{S}^* \boxtimes_{j=1}^{v} \boldsymbol{\Omega}_j^* \tag{8}$$

Note that HOSVD is performed by discarding nonzero singular values, which implies that the resulting TP model will only be an approximation. Designers need to make a careful trade-off between the complexity and the accuracy of the model, and the error can be derived based on the sum of the discarded singular values, as in the case of the HOSVD of tensors (Vannieuwenhoven et al. 2012). Thus, new vertex models and GSCs can be extracted from the reduced system tensor $\mathcal{S}^*$ and the coefficient tensor $\boldsymbol{\Omega}_i^*$ (Baranyi 2016); then an updated polytopic model is given by

$$\Delta \dot{\boldsymbol{x}} = \sum_{i=1}^{l} \alpha_i^*(\boldsymbol{\lambda}) [\boldsymbol{A}_i^* \Delta \boldsymbol{x} + \boldsymbol{B}_i^* \Delta \boldsymbol{u} + \boldsymbol{f}_{0_i}^*] \tag{9}$$

where l is the number of vertices, which is far less than the original number of local models $\Pi_{i=1}^{v} k_i$ in Eq. (4). $\boldsymbol{A}_i^*$, $\boldsymbol{B}_i^*$, and $\boldsymbol{f}_{0_i}^*$ represent the vertex matrices calculated by HOSVD. Each of the original local models can be expressed by a linear combination of the vertex models, i.e.

$$[\boldsymbol{A}_{\#}, \quad \boldsymbol{B}_{\#}, \quad \boldsymbol{f}_{0_{\#}}] \in \Omega \triangleq \mathrm{Co}\{[\boldsymbol{A}_1^*, \quad \boldsymbol{B}_1^*, \quad \boldsymbol{f}_{0_1}^*], \ldots, [\boldsymbol{A}_l^*, \quad \boldsymbol{B}_l^* \quad \boldsymbol{f}_{0_l}^*]\} \tag{10}$$

$\alpha_i^*(\boldsymbol{\lambda})$ in Eq. (9) is the unknown GSC of the reduced LPV model and satisfies the following constraints:

$$\sum_{i=1}^{l} \alpha_i^*(\boldsymbol{\lambda}) = 1 \tag{11a}$$

$$\alpha_i^*(\boldsymbol{\lambda}) \geq 0, \quad \forall \ i \tag{11b}$$

Thus, the parameters to be determined are $\boldsymbol{\alpha}^* \in \mathbb{R}^l$, which will greatly reduce the computational complexity of online identification.

Left Wing Tip Loss Case

To illustrate the efficiency of the proposed model, the authors take the left wing tip loss of the GTM in Ouellette (2010) as an example. The variable $\boldsymbol{\lambda}$ in this case represents the percentage of the wing tip loss to the semispan of the aircraft. A 10-node equally spaced grid is created over the range of $\boldsymbol{\lambda} \in [0, 33]$, corresponding to a nominal case and 9 damage cases with increasing damage severity. The HOSVD method then effectively reduces the 10 local models to a polytope with only 3 vertices, and the error of the reduction, which is defined as the maximal 2-norm of the relative differences, is within 10^{-3} (Xu et al. 2015). The 10 local models and 3 vertex models are listed in the Appendix.

Together with the vertex matrices, the HOSVD method also produces the corresponding GSC function $\boldsymbol{\alpha}^*(\boldsymbol{\lambda}) = [\alpha_1^*(\boldsymbol{\lambda}), \alpha_2^*(\boldsymbol{\lambda}), \alpha_3^*(\boldsymbol{\lambda})]^{\top}$ for the LPV model, as shown in Fig. 1. Note that one cannot use $\boldsymbol{\alpha}^*(\boldsymbol{\lambda})$ directly in the controller since $\boldsymbol{\lambda}$ is unmeasurable.

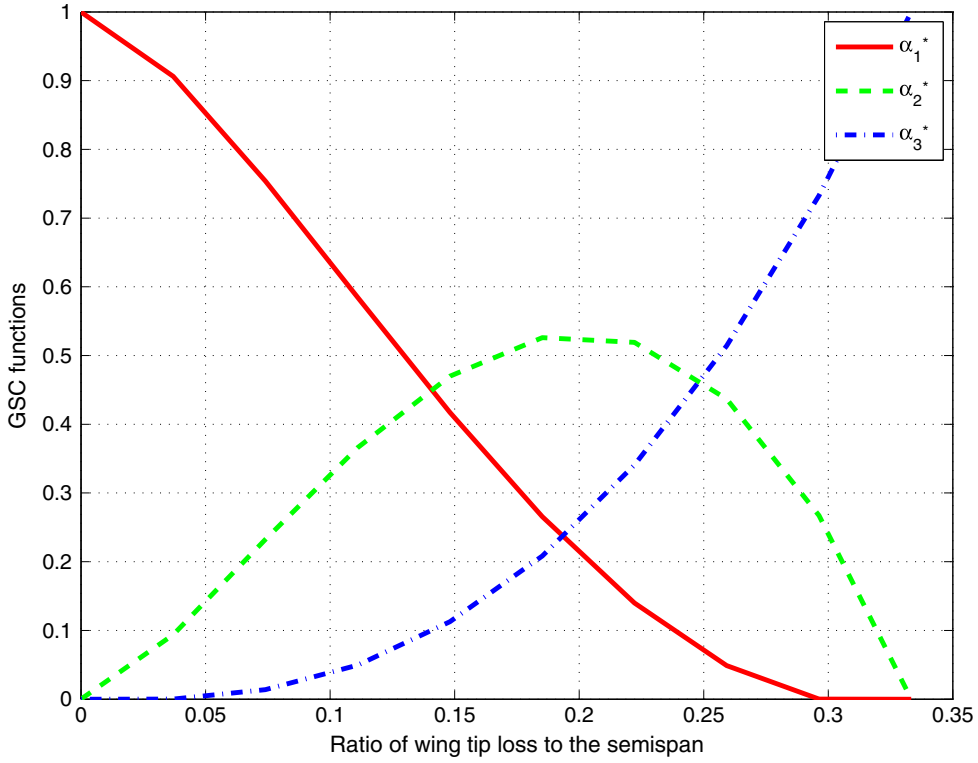

Fig. 1. GSC functions in reduced polytopic LPV model of GTM with left wing tip damage.

Table 1. Comparison of number of estimated parameters

Method	Number of estimated parameters	Explanation
LPVM-MIAC	3	GSC vector
	8	Compensation vector
ANN	3×3	Angular rate uncertainty matrix
	3×4	Trim parameter uncertainty matrix
	3×3	High-frequency gain matrix
MMRAC	3×8	State feedback matrix
	3×3	Input matrix
	3	Compensation vector

The number of estimated parameters in the LPVM-MIAC method is compared with those in the ANN method in Nguyen et al. (2008) and the MMRAC method in Guo and Tao (2015). The results are presented in Table 1. Note that an n-dimensional compensation vector is also considered in the LPVM-MIAC method, which will be presented in the next section. It is found that the LPV model has the advantage of reducing the number of estimated parameters and in turn effectively reducing the workload and complexity of the estimation.

LPV Model–Based Multivariable Indirect Adaptive Control

Considering the minor modeling errors in Eqs. (3) and (8), a mismatch term $\boldsymbol{d}$ is added to the LPV model:

$$\Delta\dot{\boldsymbol{x}} = \sum_{i=1}^{l} \alpha_i^*(\boldsymbol{\lambda})[\boldsymbol{A}_i^*\Delta\boldsymbol{x} + \boldsymbol{B}_i^*\Delta\boldsymbol{u} + \boldsymbol{f}_{0_i}^*] + \boldsymbol{d} \tag{12}$$

Thus, a multivariable indirect adaptive controller is proposed whose structure is illustrated in Fig. 2.

As shown in Fig. 2, offline-calculated vertex models of LPV are introduced into a traditional indirect adaptive control scheme. Then an online parameter identification block estimates the parameters of the LPV model, i.e., the GSC $\hat{\boldsymbol{\alpha}}^*(\boldsymbol{\lambda})$ and the compensation term $\hat{\boldsymbol{d}}$. Given the estimation, a linear system $[\hat{\boldsymbol{A}} \quad \hat{\boldsymbol{B}} \quad \hat{\boldsymbol{f}}_0 \quad \hat{\boldsymbol{d}}]$ is then formulated from the polytopic LPV model in Eq. (12). The identified system is subsequently used in the design of a model reference controller. The identification and the controller design procedures are discussed in detail in what follows.

Constrained Online Identification of LPV Model

According to the constraint in Eq. (11a)

$$\alpha_1^*(\boldsymbol{\lambda}) = 1 - \sum_{i=2}^{l} \alpha_i^*(\boldsymbol{\lambda}) \tag{13}$$

then Eq. (9) can be rewritten as

$$\Delta\dot{\boldsymbol{x}} = \left(1 - \sum_{i=2}^{l} \alpha_i^*(\boldsymbol{\lambda})\right)\left(\boldsymbol{A}_1^*\Delta\boldsymbol{x} + \boldsymbol{B}_1^*\Delta\boldsymbol{u} + \boldsymbol{f}_{0_1}^*\right) + \sum_{i=2}^{l} \alpha_i^*(\boldsymbol{\lambda})(\boldsymbol{A}_i^*\Delta\boldsymbol{x} + \boldsymbol{B}_i^*\Delta\boldsymbol{u} + \boldsymbol{f}_{0_i}^*) + \boldsymbol{d} \tag{14}$$

By defining $\boldsymbol{\theta} = [\alpha_2^*(\boldsymbol{\lambda}), \ldots, \alpha_l^*(\boldsymbol{\lambda}), \boldsymbol{d}^\top]^\top \in \mathbb{R}^{l-1+n}$ as the unknown parameter, Eq. (14) can be reformulated as

$$\Delta\dot{\boldsymbol{x}} - \boldsymbol{A}_1^*\Delta\boldsymbol{x} - \boldsymbol{B}_1^*\Delta\boldsymbol{u} - \boldsymbol{f}_{0_1}^* = \boldsymbol{\Phi}\boldsymbol{\theta} \tag{15}$$

where $\boldsymbol{\Phi} = [(\boldsymbol{A}_2^* - \boldsymbol{A}_1^*)\Delta\boldsymbol{x} + (\boldsymbol{B}_2^* - \boldsymbol{B}_1^*)\Delta\boldsymbol{u} + (\boldsymbol{f}_{0_2}^* - \boldsymbol{f}_{0_1}^*), \ldots, (\boldsymbol{A}_l^* - \boldsymbol{A}_1^*)\Delta\boldsymbol{x} + (\boldsymbol{B}_l^* - \boldsymbol{B}_1^*)\Delta\boldsymbol{u} + (\boldsymbol{f}_{0_l}^* - \boldsymbol{f}_{0_1}^*), \boldsymbol{I}_n] \in \mathbb{R}^{n\times(l-1+n)}$, and $\boldsymbol{I}_n \in \mathbb{R}^{n\times n}$ is an identity matrix.

Since one does not have direct access to the state derivatives, a low-pass filter $\boldsymbol{F}(s)$ is applied to each of the state and input signals, and its differential form $sF(s)$ is used to estimate the state derivatives; then a filtered linear system is obtained as

$$\boldsymbol{z} = \boldsymbol{\Phi}^*\boldsymbol{\theta} \tag{16}$$

where $\boldsymbol{z} = s\boldsymbol{F}_n(s)\Delta\boldsymbol{x} - (\boldsymbol{A}_1^*\boldsymbol{F}_n(s)\Delta\boldsymbol{x} + \boldsymbol{B}_1^*\boldsymbol{F}_m(s)\Delta\boldsymbol{u} + \boldsymbol{F}_n(s)\boldsymbol{f}_{0_1}^*)$ and $\boldsymbol{\Phi}^* = \boldsymbol{F}_{n+m}(s)\boldsymbol{\Phi}$, in which $\boldsymbol{F}_i(s)$ is an $i \times i$ diagonal transfer matrix, and each of its diagonal elements is $\boldsymbol{F}(s)$. Careful selection of the bandwidth of the low-pass filter allows one to suppress noise amplification to the greatest extent.

Given data of $\boldsymbol{\Phi}^*$ and $\boldsymbol{z}$ at each time instant, the estimation of parameter $\boldsymbol{\theta}$ in Eq. (16) forms a linear regression problem that can be recursively solved using a standard linear least-squares procedure. An approximation through the least-mean-squares algorithm in Åström and Wittenmark (1995) is applied, i.e.

$$\frac{\mathrm{d}\hat{\boldsymbol{\theta}}}{\mathrm{d}t} = -\boldsymbol{\Gamma}_\theta\boldsymbol{\Phi}^{*\top}\boldsymbol{\Gamma}_z\boldsymbol{\epsilon} \tag{17}$$

where $\hat{\boldsymbol{\theta}}$ denotes the estimation of $\boldsymbol{\theta}$, $\boldsymbol{\Gamma}_\theta$, and $\boldsymbol{\Gamma}_z$ are diagonal positive definite weighting matrices, and $\boldsymbol{\epsilon}$ is the estimation error of $\boldsymbol{z}$ defined as

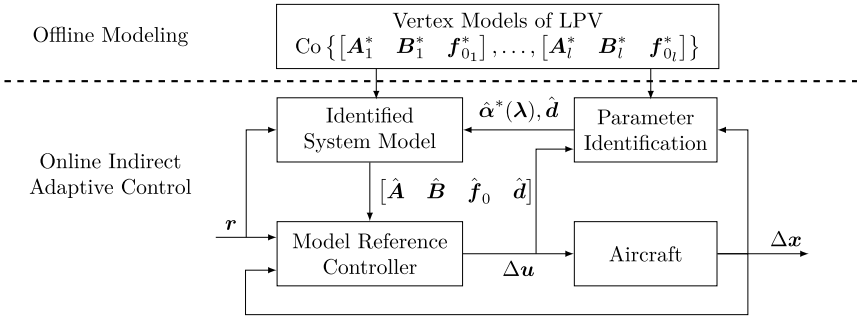

Fig. 2. Structure of LPVM-MIAC scheme.

$$\boldsymbol{\epsilon} = \frac{\boldsymbol{\Phi}^*\hat{\boldsymbol{\theta}} - z}{\|\Delta\boldsymbol{x}\|_2 + \|\Delta\boldsymbol{u} - \boldsymbol{K}_3\|_2 + c} \tag{18}$$

in which c is a small constant to prevent singularities when the magnitudes of $\Delta\boldsymbol{x}$ and $\Delta\boldsymbol{u} - \boldsymbol{K}_3$ are small. $\boldsymbol{K}_3$ is the disturbance rejection term of the controller, which will be discussed in detail in the next subsection.

Defining the estimation error as $\bar{\boldsymbol{\theta}} = \hat{\boldsymbol{\theta}} - \boldsymbol{\theta}$, one can write its time derivative as

$$\frac{\mathrm{d}\bar{\boldsymbol{\theta}}}{\mathrm{d}t} = \frac{-\boldsymbol{\Gamma}_\theta \boldsymbol{\Phi}^{*\top} \boldsymbol{\Gamma}_z \boldsymbol{\Phi}^* \bar{\boldsymbol{\theta}}}{\|\Delta\boldsymbol{x}\|_2 + \|\Delta\boldsymbol{u} - \boldsymbol{K}_3\|_2 + c} \tag{19}$$

Given a Lyapunov function

$$V(\bar{\boldsymbol{\theta}}) = \frac{1}{2}\bar{\boldsymbol{\theta}}^\top \boldsymbol{\Gamma}_\theta^{-1} \bar{\boldsymbol{\theta}} \tag{20}$$

the time derivative of $V(\bar{\boldsymbol{\theta}})$ yields

$$\begin{aligned} \frac{\mathrm{d}V(\bar{\boldsymbol{\theta}})}{\mathrm{d}t} &= -\frac{\bar{\boldsymbol{\theta}}^\top \boldsymbol{\Phi}^{*\top} \boldsymbol{\Gamma}_z \boldsymbol{\Phi}^* \bar{\boldsymbol{\theta}}}{\|\Delta\boldsymbol{x}\|_2 + \|\Delta\boldsymbol{u} - \boldsymbol{K}_3\|_2 + c} \\ &= -\frac{\sum_{i=1}^{n} \boldsymbol{\Gamma}_{z_i} (\sum_{j=1}^{l} \boldsymbol{\Phi}_{ij}^* \bar{\alpha}_j^* + \bar{d}_i)^2}{\|\Delta\boldsymbol{x}\|_2 + \|\Delta\boldsymbol{u} - \boldsymbol{K}_3\|_2 + c} \le 0 \end{aligned} \tag{21}$$

where $\boldsymbol{\Phi}_{ij}^*$ is the (i, j)th entry of $\boldsymbol{\Phi}^*$.

Remark 1: Note that $\boldsymbol{\Phi}^*$ is a time-varying function of $\Delta\boldsymbol{x}$ and $\Delta\boldsymbol{u}$, and $[\Delta\boldsymbol{x}, \Delta\boldsymbol{u}] = \boldsymbol{0}$ cannot be a trim status owing to the serious damage; therefore, $\dot{V}(\bar{\boldsymbol{\theta}})$ is negative semidefinite but not identically equal to zero except for the only equilibrium state $\bar{\boldsymbol{\theta}} = 0$. Then, according to the Lyapunov stability criterion (Khalil 1996), the estimation error $\bar{\boldsymbol{\theta}}$ is asymptotically stable and will converge to zero (Ioannou and Sun 2012).

Remark 2: Lacking persistence of excitation (PE) is not a serious problem for the aircraft damage scenario. In fact, owing to changes in the trim point, system dynamics, the strong disturbance, and the unmatched controller outputs (in the learning period), the system will be continually stimulated until it reaches another stable state.

Note that the inequality constraint in Eq. (11*b*) is not explicitly addressed and may be temporally violated in the identification procedure, but it will not affect the stability and convergence of Eq. (19).

Model Reference Controller

The following assumptions are made for designing the controller:

1. The system remains within the linear area around the operating point;
2. The impaired system has enough control capability to maintain its status; and
3. The system commands are within the control capability.

Suppose that the output of the system is given by

$$\Delta\boldsymbol{y} = \boldsymbol{C}\Delta\boldsymbol{x} \tag{22}$$

where $\Delta\boldsymbol{y} \in \mathbb{R}^w$, and it is assumed that $w \le m$, i.e., the system could be decoupled. Note that the matrix $\boldsymbol{C} \in \mathbb{R}^{w\times n}$ is an indexing matrix that extracts elements from the state vector $\Delta\boldsymbol{x}$; thus, $\boldsymbol{C}$ is not affected by changes in the characteristics of the aircraft. The goal here is to design an attitude controller that can track the predesigned reference model as

$$\boldsymbol{H}_d(s) = \begin{bmatrix} \frac{k_{1,0}}{s^{d_1+1} + k_{1,d_1}s^{d_1} + \cdots + k_{1,0}} & & \\ & \ddots & \\ & & \frac{k_{m,0}}{s^{d_m+1} + k_{m,d_m}s^{d_m} + \cdots + k_{m,0}} \end{bmatrix} \tag{23}$$

Note that $\boldsymbol{H}_d(s)$ should match the control capability of the impaired system. A slower reference model is expected in a severe damage situation or in some crucial phase, such as landing.

A state-feedback decoupling method is used to design a controller based on the identified parameters and to make the closed-loop system fulfill the desired dynamics (Guo et al. 2011; Gilbert 1969). First, a pseudo-control input $\boldsymbol{u}_p \in \mathbb{R}^w$ is introduced that has the same dimensions as the output of the system in Eq. (9)

$$\Delta\boldsymbol{u} = \boldsymbol{M}\boldsymbol{u}_p \tag{24}$$

where $\boldsymbol{M} \in \mathbb{R}^{m\times w}$ is a predesigned control allocation matrix, which maps $\boldsymbol{u}_p$ to the actual input $\Delta\boldsymbol{u}$. Then a model reference controller can be formed as a state-feedback decoupling controller (Guo et al. 2011; Gilbert 1969) with a disturbance rejection term, i.e.

$$\boldsymbol{u}_p = \boldsymbol{K}_1\Delta\boldsymbol{x} + \boldsymbol{K}_2\boldsymbol{r} + \boldsymbol{K}_3 \tag{25}$$

where $\boldsymbol{r} \in \mathbb{R}^w$, $\boldsymbol{K}_1\Delta\boldsymbol{x} + \boldsymbol{K}_2\boldsymbol{r}$ serves as the decoupling controller, and $\boldsymbol{K}_3$ implements zero-offset output tracking by canceling the effect of the $\boldsymbol{f}_0$ and $\boldsymbol{d}$ in Eq. (9). Detailed design procedures can be found in Gilbert (1969) and Guo et al. (2011), and a brief summary of the equations used is presented in what follows.

Define matrix $\boldsymbol{E}$ as

$$\boldsymbol{E} = [\boldsymbol{e}_1^\top, \quad \boldsymbol{e}_2^\top, \quad \ldots, \quad \boldsymbol{e}_w^\top]^\top \tag{26}$$

where row vector $\boldsymbol{e}_i = \boldsymbol{c}_i^\top \hat{\boldsymbol{A}}^{d_i}\hat{\boldsymbol{B}}\boldsymbol{M}$, $i = 1, \ldots, w$, and row vector $\boldsymbol{c}_i^\top$ denotes the ith row of matrix $\boldsymbol{C}$. d_i satisfies the following conditions:

$$\boldsymbol{c}_i^\top \hat{\boldsymbol{A}}^{d_i}\hat{\boldsymbol{B}}\boldsymbol{M} \neq \boldsymbol{0} \tag{27a}$$

$$\boldsymbol{c}_i^\top \hat{\boldsymbol{B}}\boldsymbol{M} = \boldsymbol{c}_i^\top \hat{\boldsymbol{A}}\,\hat{\boldsymbol{B}}\,\boldsymbol{M} = \cdots = \boldsymbol{c}_i^\top \hat{\boldsymbol{A}}^{d_i-1}\hat{\boldsymbol{B}}\boldsymbol{M} = \boldsymbol{0} \tag{27b}$$

Then the two gains of the controller can be written

$$\boldsymbol{K}_1 = -\boldsymbol{E}^{-1}\begin{bmatrix} \boldsymbol{c}_1^\top(\hat{\boldsymbol{A}}^{d_1+1} + k_{1,d_1}\hat{\boldsymbol{A}}^{d_1} + \cdots + k_{1,0}\boldsymbol{I}) \\ \boldsymbol{c}_2^\top(\hat{\boldsymbol{A}}^{d_2+1} + k_{2,d_2}\hat{\boldsymbol{A}}^{d_2} + \cdots + k_{2,0}\boldsymbol{I}) \\ \vdots \\ \boldsymbol{c}_w^\top(\hat{\boldsymbol{A}}^{d_w+1} + k_{w,d_w}\hat{\boldsymbol{A}}^{d_w} + \cdots + k_{w,0}\boldsymbol{I}) \end{bmatrix} \tag{28a}$$

$$\boldsymbol{K}_2 = -\boldsymbol{E}^{-1}\begin{bmatrix} k_{1,0} & & & \\ & k_{2,0} & & \\ & & \ddots & \\ & & & k_{w,0} \end{bmatrix} \tag{28b}$$

The computation of $\boldsymbol{K}_3$ follows from the idea in Guo et al. (2011), which makes the steady-state gain of the transfer function from $\boldsymbol{f}_0 + \boldsymbol{d}$ to $\Delta\boldsymbol{y}$ equal 0, i.e.

$$\lim_{s\to 0} s\boldsymbol{C}(s\boldsymbol{I} - \hat{\boldsymbol{A}} - \hat{\boldsymbol{B}}\boldsymbol{M}\boldsymbol{K}_1)^{-1}\left(\hat{\boldsymbol{B}}\boldsymbol{M}\frac{\boldsymbol{K}_3}{s} + \frac{\hat{\boldsymbol{f}}_0 + \hat{\boldsymbol{d}}}{s}\right) = 0 \tag{29}$$

Solving the preceding equation yields

$$\boldsymbol{K}_3 = -[\boldsymbol{C}(\hat{\boldsymbol{A}} + \hat{\boldsymbol{B}}\boldsymbol{M}\boldsymbol{K}_1)^{-1}\hat{\boldsymbol{B}}\boldsymbol{M}]^{-1}\boldsymbol{C}(\hat{\boldsymbol{A}} + \hat{\boldsymbol{B}}\boldsymbol{M}\boldsymbol{K}_1)^{-1}(\hat{\boldsymbol{f}}_0 + \hat{\boldsymbol{d}}) \tag{30}$$

Case Study: Left Wing Tip Loss of GTM

In this section, the proposed LPVM-MIAC method is tested on the simulation model of the NASA GTM. The GTM is a 5.5% dynamically scaled, remotely piloted, twin-turbine aircraft model that serves as a testbed for dynamics modeling and advanced flight control experiments. Along with the physical GTM is a MATLAB/Simulink model. This high-fidelity nonlinear simulation model includes several adverse flight conditions, such as high angle of attack, structural damage, and so forth. Actuator dynamics with position and slew rate saturation and sensor dynamics are also incorporated into the model (Jordan et al. 2004). The dynamics of the actuators is also considered, which is a second-order system with the damping ratio as $\zeta = 0.7$ and the natural frequency as $\omega_n = 40$ rad/s.

An attitude controller is designed for a prespecified operating point of the aircraft. At the operating point, the airspeed is 46.3 m/s, the angle of attack and pitch angle are 4.096°, and the altitude is 304.8 m. All other state variables are 0. The loss of the left wing tip scenario is considered. The parameters of the controllers are listed as follows, where diag() creates a diagonal matrix from a vector and $\boldsymbol{I}_n$ denotes an identity matrix in $\mathbb{R}^{n\times n}$:

$$\begin{aligned} \boldsymbol{\Gamma}_\theta &= \mathrm{diag}([0.6, 0.01, 500, 500, 500, 500, 500, 500, 500, 500]) \\ \boldsymbol{\Gamma}_z &= \mathrm{diag}([30, 10, 1, 30, 30, 1, 1, 30]) \\ c &= 20 \\ \boldsymbol{H}_d(s) &= \frac{9}{s^2 + 4.8s + 9}\boldsymbol{I}_3 \\ F(s) &= \frac{1}{0.3s + 1} \end{aligned} \tag{31}$$

A 40-s simulation with attitude commands as illustrated in Fig. 3 is performed. A 20% damage of the left wing tip occurs at 10 s after the simulation begins.

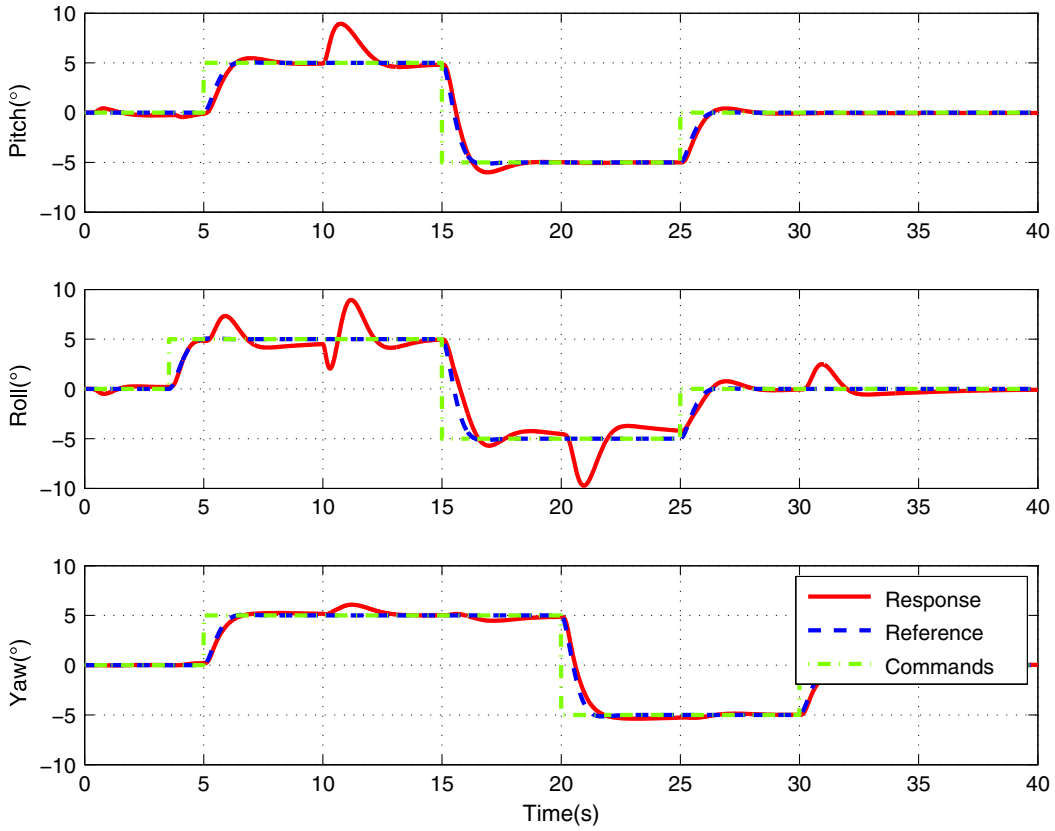

Fig. 3. Attitude commands, references generated by reference model, and responses of aircraft model.

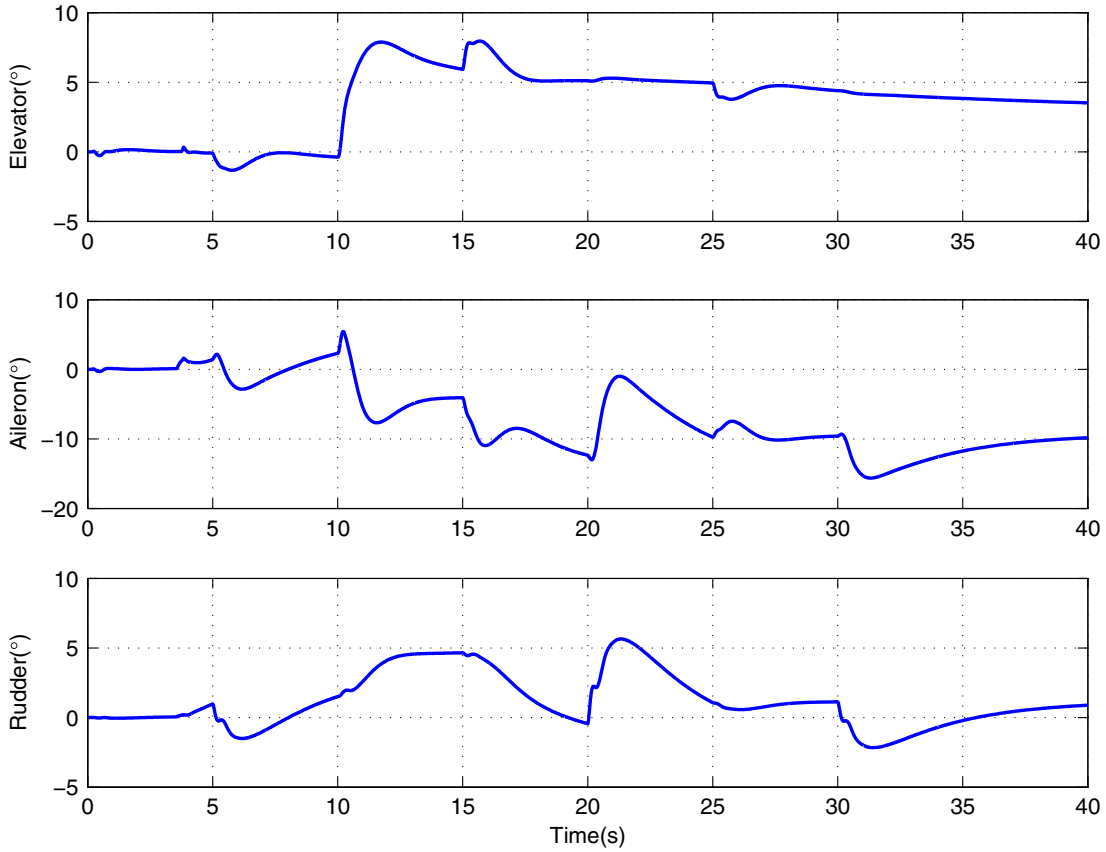

Fig. 4. Control inputs.

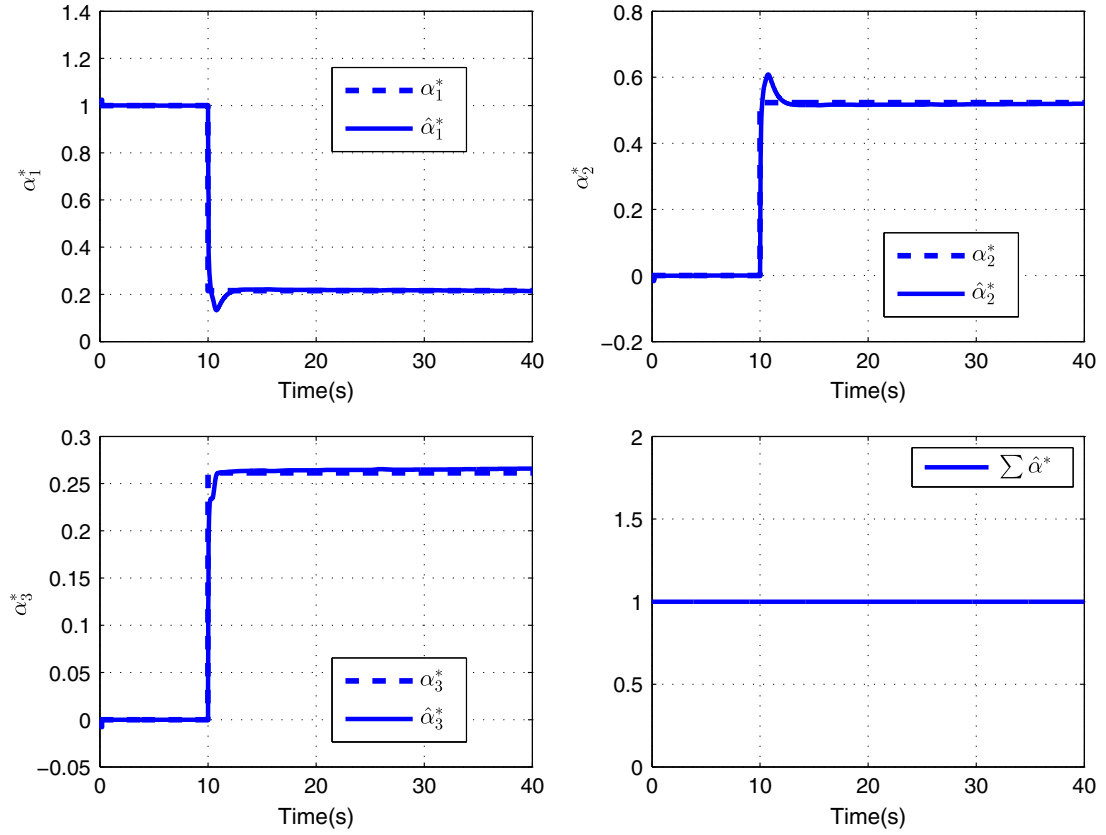

Fig. 5. GSC estimation.

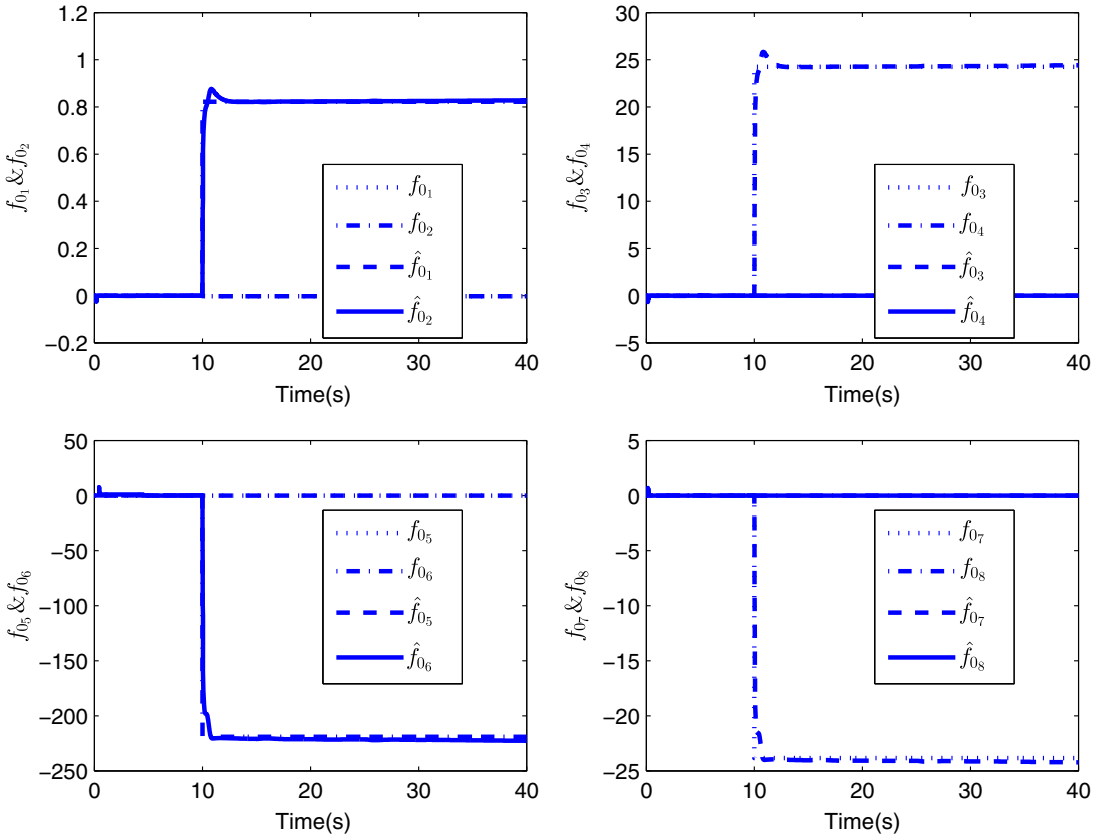

Fig. 6. Disturbance estimation.

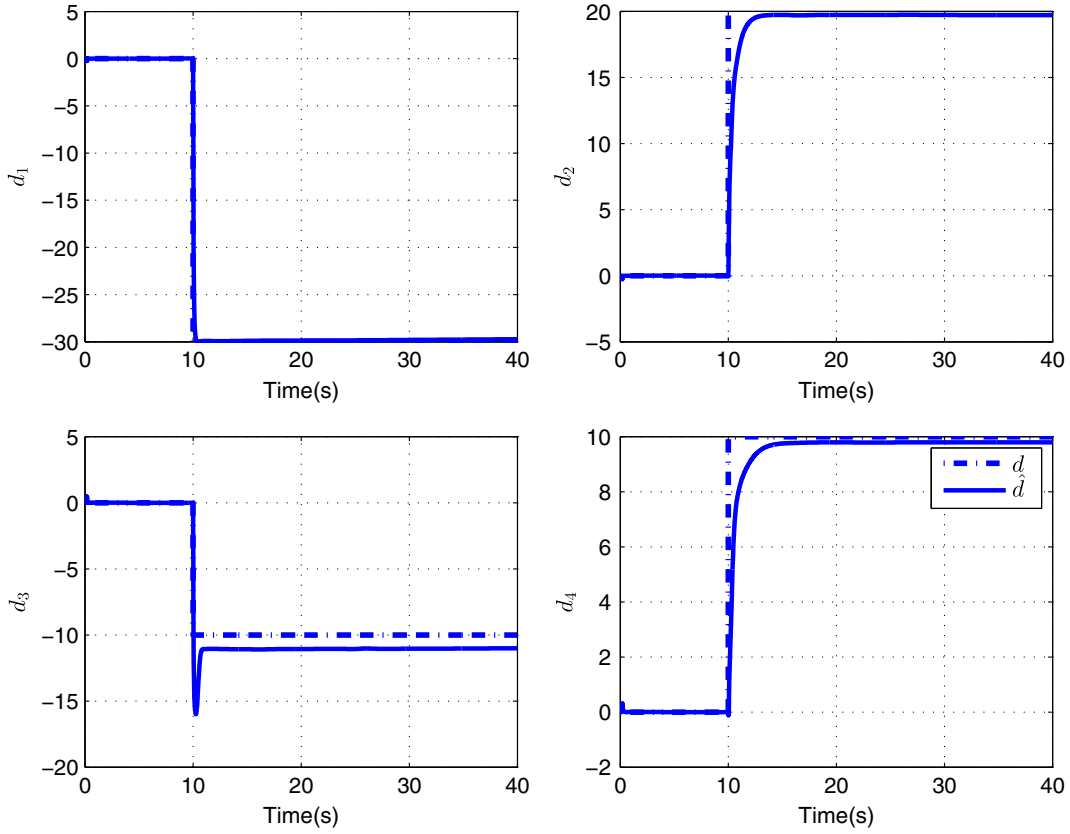

Fig. 7. Uncertainty estimation.

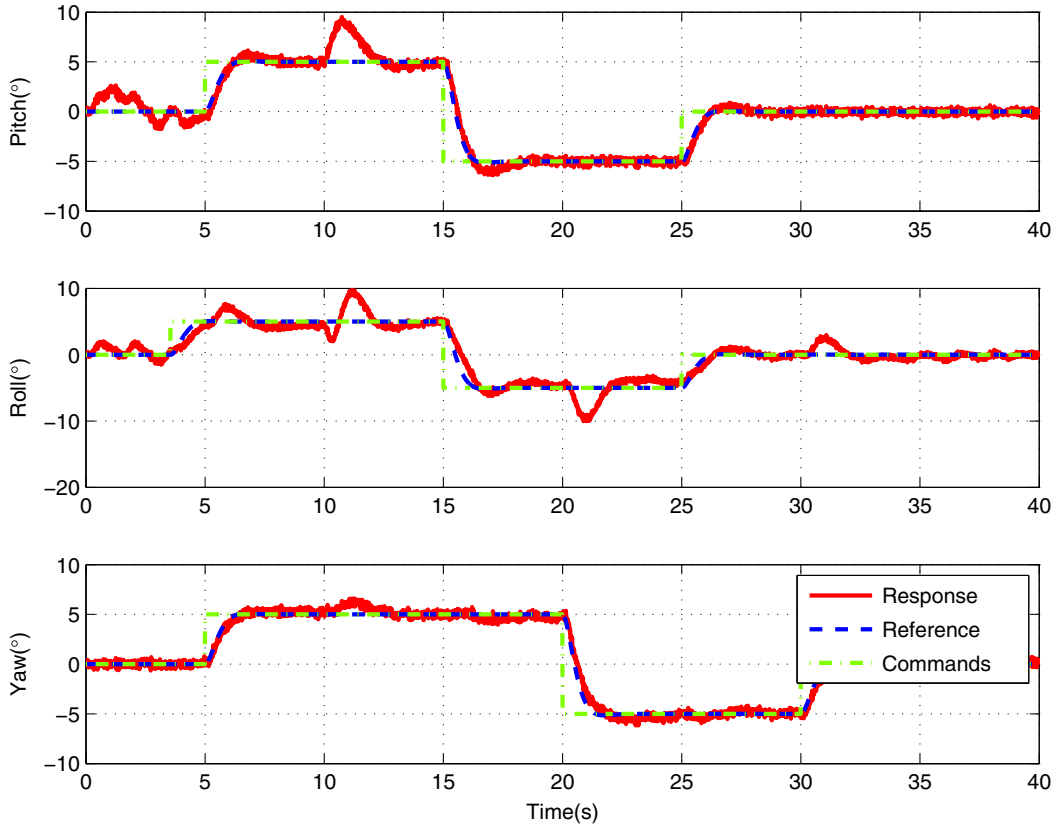

Fig. 8. Attitude commands, attitude references generated by reference model, and responses of aircraft model under measurement noises.

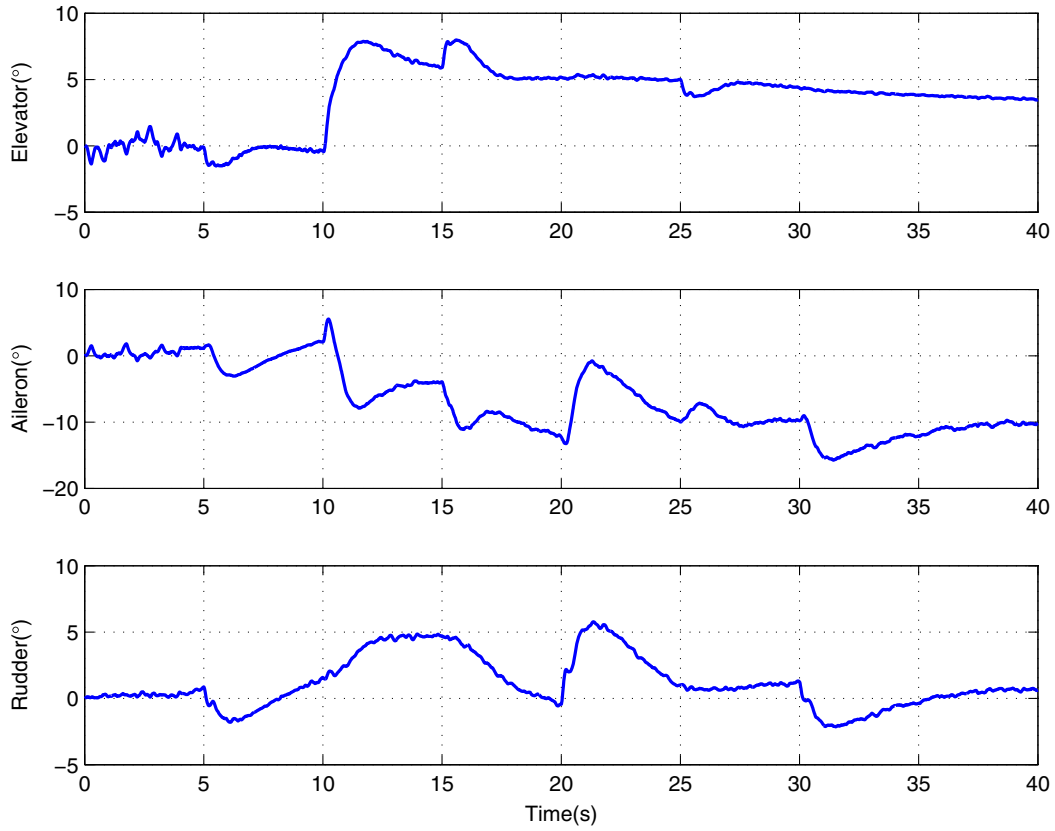

Fig. 9. Control inputs under measurement noises.

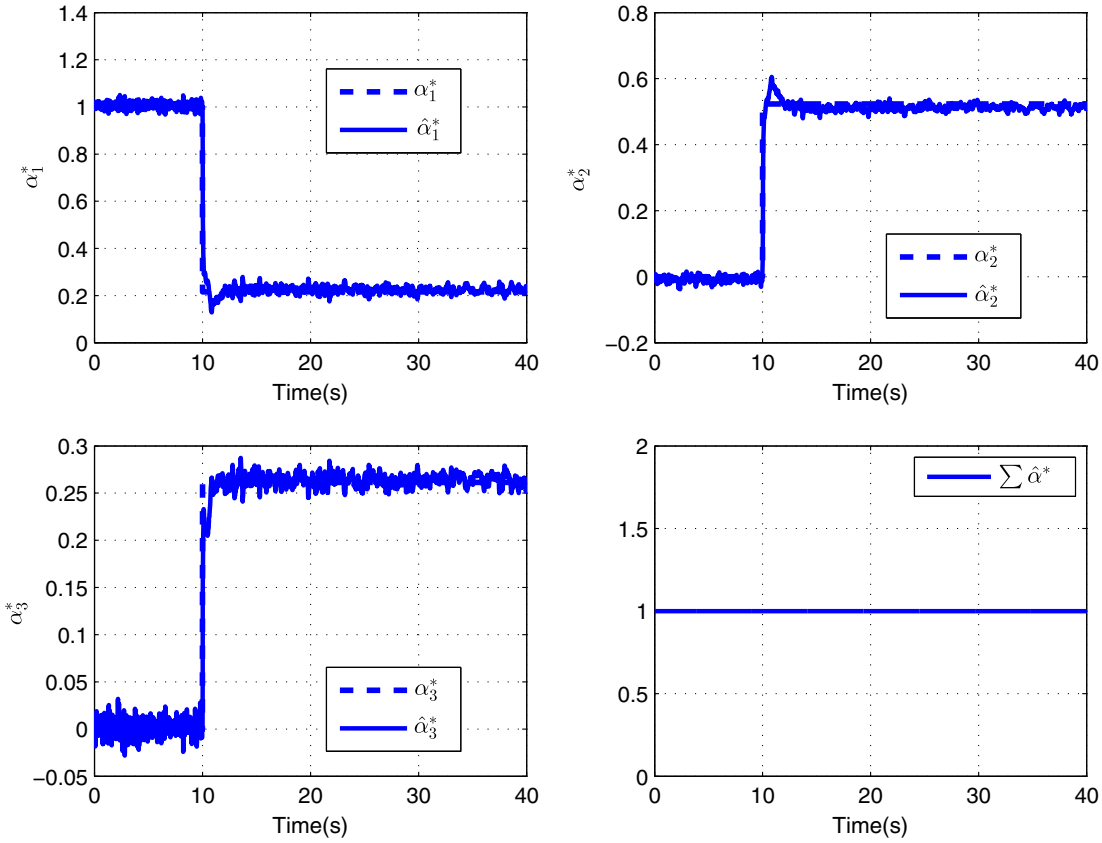

Fig. 10. GSC estimation under measurement noises.

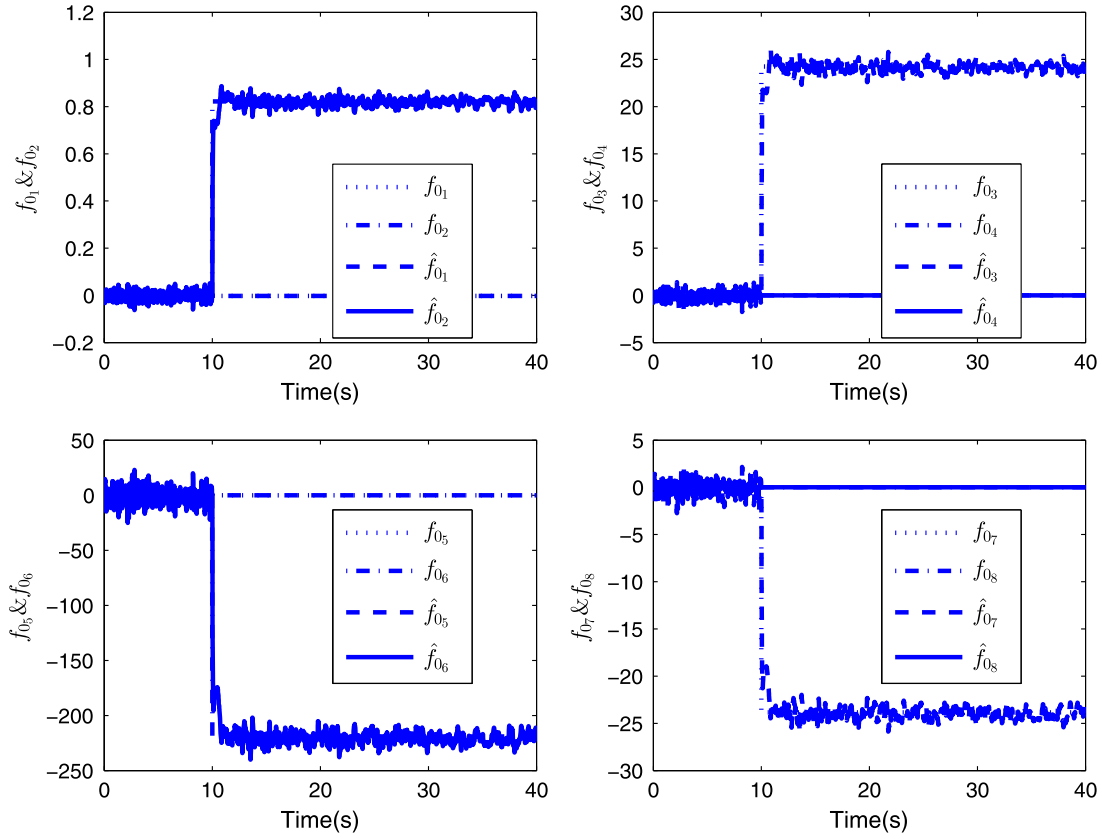

Fig. 11. Disturbance estimation under measurement noises.

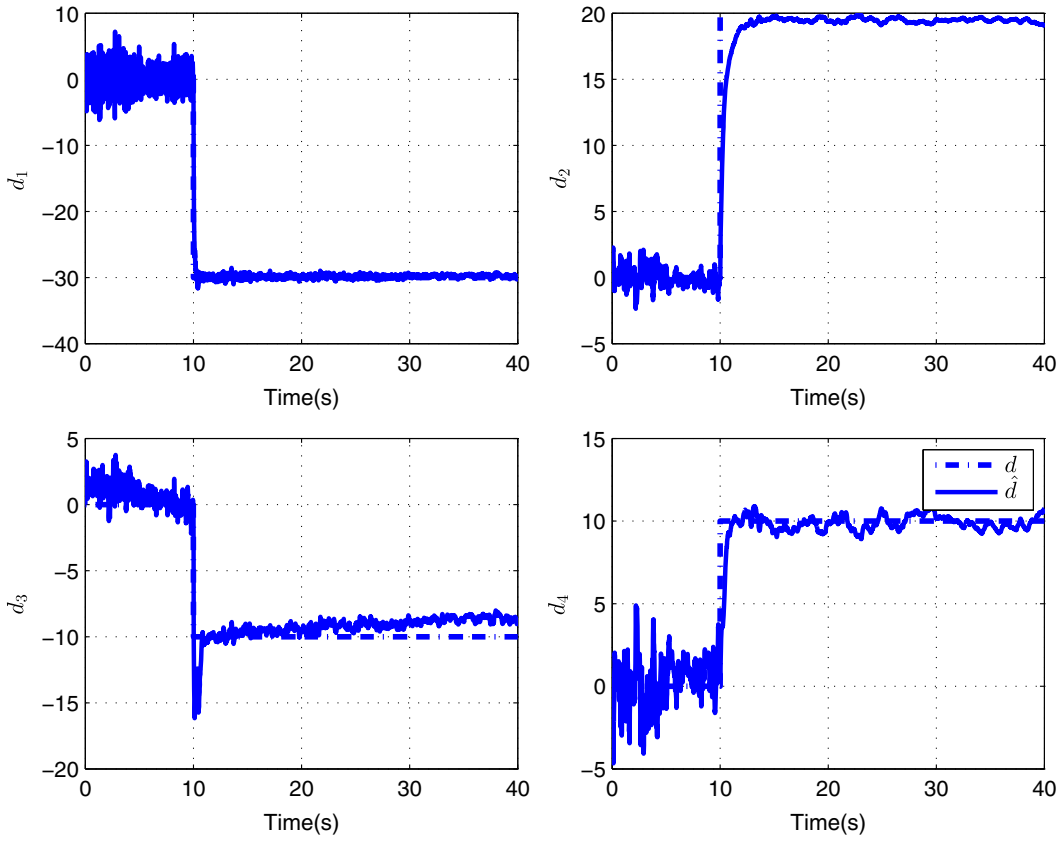

Fig. 12. Uncertainty estimation under measurement noises.

To clearly show the transient and tracking responses of aircraft states, a simulation without state measurement noise is performed first, and the results are shown in Figs. 3–6.

Fig. 3 shows the attitude commands and responses of the aircraft model along with the output of the reference models. As shown, before 10 s, the responses of the aircraft closely track those of the reference models. This is the result of a particular choice of the initial GSCs, which makes the LPV model approximate the actual dynamics of the aircraft and saves the controller from substantial adaptation. When the damage occurs at 10 s, a temporary oscillation appears in the attitude angles, which is an indication of the adaptation of the controller. The oscillation dies out quickly in approximately 3 s, and the tracking of the attitude angles recovers, leading to a consistency between the response and the reference. Note that a sudden aggravation occurred in the roll channel from 20 to 23 s, which was due to the yaw command at 20 s, and the aircraft performs a bank turn maneuver.

The corresponding control inputs are depicted in Fig. 4. As shown, during attitude control, the ailerons are used to compensate for the effect of the wing tip damage, and the movements of all the control surfaces are within the physical limits of the actuators.

The adaptation of the GSCs, $\boldsymbol{f}_0$, and $\boldsymbol{d}$ are shown in Figs. 5–7. When the damage occurs, the estimated parameters adjust rapidly and converge stably to the true values. The sum of the GSCs satisfies the equality constraints in Eqs. (11*a*) and (11*b*).

To make the simulation more realistic, Gaussian measurement noises are added to the state variables, with zero mean and variance of $[1, 0.01, 0.005, 0.05, 0.1, 0.005, 0.005, 0.05]$. The simulation results are shown in Figs. 8–12.

As shown, the results are similar to those without noise. In other words, the controller is robust to a reasonable noise level, which reflects the applicability of the proposed control method under practical applications.

Conclusions

A damaged asymmetric aircraft represents a severe case in which aircraft handling quality and flight safety are significantly affected, posing challenges for the design of flight control systems. By incorporating an offline analysis of the dynamics of the damaged aircraft, a reduced-sized LPV model with sufficient accuracy is constructed. A model reference controller is designed based on this LPV model, implementing both the matching of the ideal closed-loop dynamics and offset-free tracking. Simulations of attitude control on the NASA GTM demonstrate the effectiveness of the method, i.e., the identified coefficients of the LPV model quickly converge as the damage occurs, and the controller achieves satisfactory tracking of the attitude angles in both noise-free and noisy state measurements. A future research topic will be to focus on a system with damage at different operating points, such as different angles of attack, heights, and Mach numbers. Moreover, the authors' research will be extended to LPV modeling and identification with hybrid measurable/unmeasurable GSCs.

Appendix. LPV Model

The 10 local models $[\boldsymbol{A}_i \quad \boldsymbol{B}_i \quad \boldsymbol{f}_{0_i}](i = 1 \ldots 10)$ and 3 vertex models $[\boldsymbol{A}_i^* \quad \boldsymbol{B}_i^* \quad \boldsymbol{f}_{0_i}^*](i = 1, 2, 3)$ of the GTM are as follows:

$$[\boldsymbol{A}_1 \quad \boldsymbol{B}_1 \quad \boldsymbol{f}_{0_1}] = \begin{bmatrix} -0.0291 & 0.196 & -0.0022 & -0.171 & 0 & 0 & 0 & 0 & -0.0196 & 0 & 0 & 0 \\ -0.52 & -2.6 & 0.966 & 0 & 0 & 0 & 0 & 0 & -0.25 & 0 & 0 & 0 \\ -1.29e-05 & -29 & -3.04 & 0 & 0 & 0 & 0 & 0 & -43.3 & 0 & 0 & 0 \\ 0 & 0 & 1 & 0 & 0 & 0 & 0 & 0 & 0 & 0 & 0 & 0 \\ 0 & 0 & 0 & 0 & -0.562 & 0.0711 & -0.988 & 0.211 & 0 & 0.00959 & 0.214 & 0 \\ 0 & 0 & 0 & 0 & -75.3 & -4.66 & 0.548 & 0 & 0 & 39.6 & 11.1 & 0 \\ 0 & 0 & 0 & 0 & 24.9 & -0.393 & -1.02 & 0 & 0 & 3.28 & -28.5 & 0 \\ 0 & 0 & 0 & 0 & 0 & 1 & 0.0716 & 0 & 0 & 0 & 0 & 0 \end{bmatrix} \tag{32}$$

$$[\boldsymbol{A}_2 \quad \boldsymbol{B}_2 \quad \boldsymbol{f}_{0_2}] = \begin{bmatrix} -0.0291 & 0.196 & -0.0022 & -0.171 & 2.07e-05 & -9.32e-06 & -2.46e-06 & 0 & -0.0197 & 0.000159 & -9.53e-05 & -0.000174 \\ -0.519 & -2.59 & 0.966 & 0 & -0.000767 & -0.000178 & 8.43e-06 & 0 & -0.25 & 0.00256 & -3.66e-05 & 0.0636 \\ 0.0802 & -28.7 & -3.04 & 0 & -0.0176 & -0.00443 & 0.000137 & 0 & -43.3 & 0.0935 & -0.00371 & 1.86 \\ 0 & 0 & 1 & 0 & 0 & 0 & 0 & 0 & 0 & 0 & 0 & 0 \\ -2.48e-05 & 0.000378 & -2.2e-06 & 0 & -0.562 & 0.0711 & -0.988 & 0.211 & -2.26e-08 & 0.00945 & 0.214 & -0.00115 \\ -0.0838 & -0.348 & 0.00307 & 0 & -75.4 & -4.66 & 0.549 & 0 & 0.0506 & 39.6 & 11.2 & -1.93 \\ -0.0105 & -0.0547 & 5.98e-05 & 0 & 24.9 & -0.394 & -1.02 & 0 & 0.00175 & 3.29 & -28.6 & -0.221 \\ 0 & 0 & 0 & 0 & 0 & 1 & 0.0716 & 0 & 0 & 0 & 0 & 0 \end{bmatrix} \tag{33}$$

$$[\boldsymbol{A}_3 \quad \boldsymbol{B}_3 \quad \boldsymbol{f}_{0_3}] = \begin{bmatrix} -0.0291 & 0.196 & -0.00219 & -0.171 & -1.99e-05 & -2.62e-05 & -4.2e-06 & 0 & -0.0197 & 0.000448 & -0.000193 & -0.000493 \\ -0.516 & -2.57 & 0.966 & 0 & -0.00241 & -0.000519 & 2.54e-05 & 0 & -0.25 & 0.00736 & -7.44e-05 & 0.182 \\ 0.231 & -28.2 & -3.03 & 0 & -0.0618 & -0.0132 & 0.000519 & 0 & -43.3 & 0.27 & -0.00738 & 5.34 \\ 0 & 0 & 1 & 0 & 0 & 0 & 0 & 0 & 0 & 0 & 0 & 0 \\ -6.98e-05 & 0.00107 & -6.2e-06 & 0 & -0.562 & 0.0711 & -0.988 & 0.211 & -9.25e-08 & 0.00922 & 0.214 & -0.00323 \\ -0.685 & -3.08 & -0.00225 & 0 & -75.3 & -4.64 & 0.548 & 0 & 0.101 & 39.3 & 11.2 & -15.8 \\ -0.0771 & -0.437 & -0.000675 & 0 & 24.9 & -0.393 & -1.02 & 0 & 0.00347 & 3.27 & -28.6 & -1.74 \\ 0 & 0 & 0 & 0 & 0 & 1 & 0.0716 & 0 & 0 & 0 & 0 & 0 \end{bmatrix} \tag{34}$$

$$[\boldsymbol{A}_4 \quad \boldsymbol{B}_4 \quad \boldsymbol{f}_{0_4}] = \begin{bmatrix} -0.0291 & 0.196 & -0.00219 & -0.171 & -9.2e-05 & -4.81e-05 & -5.77e-06 & 0 & -0.0197 & 0.000822 & -0.000301 & -0.000912 \\ -0.513 & -2.54 & 0.966 & 0 & -0.0046 & -0.000965 & 4.77e-05 & 0 & -0.25 & 0.0136 & -0.000116 & 0.337 \\ 0.427 & -27.5 & -3.03 & 0 & -0.123 & -0.0247 & 0.00105 & 0 & -43.3 & 0.5 & -0.0112 & 9.89 \\ 0 & 0 & 1 & 0 & 0 & 0 & 0 & 0 & 0 & 0 & 0 & 0 \\ -0.000127 & 0.00198 & -1.14e-05 & 0 & -0.562 & 0.0711 & -0.988 & 0.211 & -2.23e-07 & 0.00892 & 0.214 & -0.00589 \\ -2.03 & -9.25 & -0.0194 & 0 & -75.1 & -4.59 & 0.547 & 0 & 0.156 & 38.7 & 11.2 & -47 \\ -0.225 & -1.29 & -0.00255 & 0 & 25 & -0.389 & -1.02 & 0 & 0.00529 & 3.21 & -28.6 & -5.13 \\ 0 & 0 & 0 & 0 & 0 & 1 & 0.0716 & 0 & 0 & 0 & 0 & 0 \end{bmatrix} \tag{35}$$

$$[\boldsymbol{A}_5 \quad \boldsymbol{B}_5 \quad \boldsymbol{f}_{0_5}] = \begin{bmatrix} -0.0292 & 0.195 & -0.00218 & -0.171 & -0.000181 & -7.39e-05 & -7.44e-06 & 0 & -0.0197 & 0.00127 & -0.000424 & -0.00142 \\ -0.509 & -2.5 & 0.967 & 0 & -0.00721 & -0.0015 & 7.44e-05 & 0 & -0.25 & 0.0211 & -0.000163 & 0.52 \\ 0.661 & -26.7 & -3.03 & 0 & -0.197 & -0.0385 & 0.0017 & 0 & -43.3 & 0.775 & -0.0155 & 15.3 \\ 0 & 0 & 1 & 0 & 0 & 0 & 0 & 0 & 0 & 0 & 0 & 0 \\ -0.000194 & 0.00307 & -1.74e-05 & 0 & -0.562 & 0.0711 & -0.988 & 0.211 & -4.39e-07 & 0.00856 & 0.214 & -0.00896 \\ -4.3 & -19.7 & -0.051 & 0 & -74.5 & -4.5 & 0.543 & 0 & 0.216 & 37.5 & 11.2 & -99.6 \\ -0.473 & -2.73 & -0.00582 & 0 & 25 & -0.381 & -1.02 & 0 & 0.00729 & 3.12 & -28.6 & -10.8 \\ 0 & 0 & 0 & 0 & 0 & 1 & 0.0716 & 0 & 0 & 0 & 0 & 0 \end{bmatrix} \tag{36}$$

$$[\boldsymbol{A}_6 \quad \boldsymbol{B}_6 \quad \boldsymbol{f}_{0_6}] = \begin{bmatrix} -0.0292 & 0.195 & -0.00217 & -0.171 & -0.000279 & -0.000103 & -9.42e-06 & 0 & -0.0198 & 0.00177 & -0.000565 & -0.00203 \\ -0.504 & -2.46 & 0.967 & 0 & -0.0102 & -0.0021 & 0.000105 & 0 & -0.25 & 0.0295 & -0.000218 & 0.729 \\ 0.928 & -25.7 & -3.02 & 0 & -0.282 & -0.0543 & 0.00245 & 0 & -43.3 & 1.09 & -0.0202 & 21.5 \\ 0 & 0 & 1 & 0 & 0 & 0 & 0 & 0 & 0 & 0 & 0 & 0 \\ -0.000266 & 0.00435 & -2.42e-05 & 0 & -0.562 & 0.0711 & -0.988 & 0.211 & -7.76e-07 & 0.00817 & 0.214 & -0.0123 \\ -7.65 & -35 & -0.0994 & 0 & -73.6 & -4.36 & 0.538 & 0 & 0.283 & 35.8 & 11.2 & -177 \\ -0.838 & -4.84 & -0.0107 & 0 & 25.1 & -0.37 & -1.02 & 0 & 0.00951 & 2.98 & -28.6 & -19.3 \\ 0 & 0 & 0 & 0 & 0 & 1 & 0.0716 & 0 & 0 & 0 & 0 & 0 \end{bmatrix} \tag{37}$$

$$[\boldsymbol{A}_7 \quad \boldsymbol{B}_7 \quad \boldsymbol{f}_{0_7}] = \begin{bmatrix} -0.0292 & 0.195 & -0.00215 & -0.171 & -0.000376 & -0.000136 & -1.18e-05 & 0 & -0.0198 & 0.00233 & -0.000728 & -0.00274 \\ -0.499 & -2.41 & 0.967 & 0 & -0.0135 & -0.00277 & 0.000138 & 0 & -0.251 & 0.0389 & -0.000281 & 0.962 \\ 1.23 & -24.6 & -3.02 & 0 & -0.377 & -0.0718 & 0.00328 & 0 & -43.3 & 1.43 & -0.0254 & 28.4 \\ 0 & 0 & 1 & 0 & 0 & 0 & 0 & 0 & 0 & 0 & 0 & 0 \\ -0.00034 & 0.0058 & -3.16e-05 & 0 & -0.561 & 0.0711 & -0.988 & 0.211 & -1.28e-06 & 0.00773 & 0.215 & -0.0157 \\ -12.2 & -56 & -0.167 & 0 & -72.4 & -4.17 & 0.531 & 0 & 0.36 & 33.5 & 11.2 & -282 \\ -1.33 & -7.72 & -0.0175 & 0 & 25.3 & -0.355 & -1.02 & 0 & 0.012 & 2.79 & -28.6 & -30.7 \\ 0 & 0 & 0 & 0 & 0 & 1 & 0.0716 & 0 & 0 & 0 & 0 & 0 \end{bmatrix} \tag{38}$$

$$[\boldsymbol{A}_8 \quad \boldsymbol{B}_8 \quad \boldsymbol{f}_{0_8}] = \begin{bmatrix} -0.0293 & 0.195 & -0.00214 & -0.171 & -0.000467 & -0.000171 & -1.48e-05 & 0 & -0.0199 & 0.00293 & -0.000915 & -0.00358 \\ -0.494 & -2.36 & 0.967 & 0 & -0.0171 & -0.0035 & 0.000175 & 0 & -0.251 & 0.0492 & -0.000354 & 1.22 \\ 1.55 & -23.5 & -3.01 & 0 & -0.482 & -0.0911 & 0.00419 & 0 & -43.3 & 1.81 & -0.0311 & 35.9 \\ 0 & 0 & 1 & 0 & 0 & 0 & 0 & 0 & 0 & 0 & 0 & 0 \\ -0.000413 & 0.00746 & -3.94e-05 & 0 & -0.561 & 0.0712 & -0.988 & 0.211 & -2.02e-06 & 0.00726 & 0.215 & -0.0191 \\ -18.1 & -83.1 & -0.255 & 0 & -70.7 & -3.92 & 0.521 & 0 & 0.445 & 30.5 & 11.3 & -419 \\ -1.98 & -11.4 & -0.0263 & 0 & 25.4 & -0.334 & -1.02 & 0 & 0.0148 & 2.54 & -28.7 & -45.6 \\ 0 & 0 & 0 & 0 & 0 & 1 & 0.0716 & 0 & 0 & 0 & 0 & 0 \end{bmatrix} \tag{39}$$

$$[\boldsymbol{A}_9 \quad \boldsymbol{B}_9 \quad \boldsymbol{f}_{0_9}] = \begin{bmatrix} -0.0294 & 0.194 & -0.00213 & -0.171 & -0.000545 & -0.000209 & -1.85e-05 & 0 & -0.0199 & 0.00359 & -0.00113 & -0.00458 \\ -0.488 & -2.31 & 0.968 & 0 & -0.021 & -0.00429 & 0.000214 & 0 & -0.251 & 0.0604 & -0.000437 & 1.5 \\ 1.91 & -22.2 & -3.01 & 0 & -0.596 & -0.112 & 0.00517 & 0 & -43.3 & 2.22 & -0.0374 & 44.2 \\ 0 & 0 & 1 & 0 & 0 & 0 & 0 & 0 & 0 & 0 & 0 & 0 \\ -0.000481 & 0.00936 & -4.75e-05 & 0 & -0.561 & 0.0712 & -0.988 & 0.211 & -3.05e-06 & 0.00676 & 0.215 & -0.0223 \\ -25.5 & -117 & -0.367 & 0 & -68.6 & -3.6 & 0.509 & 0 & 0.54 & 26.7 & 11.3 & -590 \\ -2.78 & -16.1 & -0.0373 & 0 & 25.6 & -0.309 & -1.03 & 0 & 0.0178 & 2.23 & -28.7 & -64.1 \\ 0 & 0 & 0 & 0 & 0 & 1 & 0.0716 & 0 & 0 & 0 & 0 & 0 \end{bmatrix} \tag{40}$$

$$[\boldsymbol{A}_{10} \quad \boldsymbol{B}_{10} \quad \boldsymbol{f}_{0_{10}}] = \begin{bmatrix} -0.0294 & 0.194 & -0.00211 & -0.171 & -0.000603 & -0.00025 & -2.28e-05 & 0 & -0.02 & 0.00428 & -0.00137 & -0.00578 \\ -0.481 & -2.25 & 0.968 & 0 & -0.0251 & -0.00515 & 0.000256 & 0 & -0.251 & 0.0723 & -0.000531 & 1.8 \\ 2.29 & -20.8 & -3 & 0 & -0.72 & -0.135 & 0.00622 & 0 & -43.3 & 2.66 & -0.0442 & 53 \\ 0 & 0 & 1 & 0 & 0 & 0 & 0 & 0 & 0 & 0 & 0 & 0 \\ -0.000536 & 0.0115 & -5.55e-05 & 0 & -0.561 & 0.0712 & -0.988 & 0.211 & -4.46e-06 & 0.00625 & 0.215 & -0.0248 \\ -34.4 & -158 & -0.503 & 0 & -66 & -3.22 & 0.494 & 0 & 0.645 & 22 & 11.3 & -797 \\ -3.76 & -21.8 & -0.0508 & 0 & 25.9 & -0.277 & -1.03 & 0 & 0.0211 & 1.85 & -28.7 & -86.7 \\ 0 & 0 & 0 & 0 & 0 & 1 & 0.0716 & 0 & 0 & 0 & 0 & 0 \end{bmatrix} \tag{41}$$

$$[\boldsymbol{A}_1^* \quad \boldsymbol{B}_1^* \quad \boldsymbol{f}_{0_1}^*] = \begin{bmatrix} -0.0291 & 0.196 & -0.0022 & -0.171 & 4.24e-05 & -6.61e-08 & 0 & 0 & -0.0196 & 5.35e-07 & -3.79e-05 & 0.0443 & 0 \\ -0.52 & -2.6 & 0.966 & 0 & 9.61e-05 & 4.38e-06 & -6.34e-07 & 0 & -0.25 & -2.61e-05 & -1.46e-05 & -0.00393 & 0 \\ -0.000167 & -29 & -3.04 & 0 & 0.00484 & 0.000212 & -5.79e-05 & 0 & -43.3 & -0.00162 & -0.00144 & 7.52e-05 & 0 \\ 0 & 0 & 1 & 0 & 0 & 0 & 0 & 0 & 0 & 0 & 0 & 0 & 0 \\ 4.91e-06 & 4.71e-05 & 0 & 0 & -0.562 & 0.0711 & -0.988 & 0.211 & 0 & 0.00958 & 0.214 & 0 & 0 \\ -0.00027 & 0.0136 & 0.00172 & 0 & -75.3 & -4.66 & 0.548 & 0 & 0.0199 & 39.6 & 11.1 & 0.000203 & 0 \\ -0.000719 & 0.00162 & 6.57e-05 & 0 & 24.9 & -0.394 & -1.02 & 0 & 0.000687 & 3.28 & -28.5 & 0.000582 & 0 \\ 0 & 0 & 0 & 0 & 0 & 1 & 0.0716 & 0 & 0 & 0 & 0 & 0 & 0 \end{bmatrix} \tag{42}$$

$$[\boldsymbol{A}_2^* \quad \boldsymbol{B}_2^* \quad \boldsymbol{f}_{0_2}^*] = \begin{bmatrix} -0.0292 & 0.195 & -0.0022 & -0.171 & -0.000297 & -9.74e-05 & 0 & 0 & -0.0198 & 0.00167 & -0.000528 & 0.0443 & -0.00154 \\ -0.506 & -2.47 & 0.967 & 0 & -0.00943 & -0.00195 & 9.77e-05 & 0 & -0.25 & 0.0275 & -0.000202 & -0.00393 & 0.674 \\ 0.857 & -26 & -3.02 & 0 & -0.251 & -0.0499 & 0.0022 & 0 & -43.3 & 1.01 & -0.0207 & 0.001 & 19.9 \\ 0 & 0 & 1 & 0 & 0 & 0 & 0 & 0 & 0 & 0 & 0 & 0 & 0 \\ -0.000295 & 0.00367 & 0 & 0 & -0.562 & 0.0711 & -0.988 & 0.211 & 0 & 0.00821 & 0.214 & 0 & -0.0137 \\ -0.889 & -3.88 & 0.0102 & 0 & -75.8 & -4.66 & 0.551 & 0 & 0.281 & 39.4 & 11.2 & 0.00278 & -20.5 \\ -0.103 & -0.589 & -0.000264 & 0 & 24.9 & -0.395 & -1.02 & 0 & 0.00964 & 3.29 & -28.6 & 0.00811 & -2.27 \\ 0 & 0 & 0 & 0 & 0 & 1 & 0.0716 & 0 & 0 & 0 & 0 & 0 & 0 \end{bmatrix} \tag{43}$$

$$
[\boldsymbol{A}_3^* \quad \boldsymbol{B}_3^* \quad \boldsymbol{f}_{0_3}^*] = \left[\begin{array}{cccccccccccccc}
-0.0294 & 0.194 & -0.0022 & -0.171 & -0.000623 & -0.00025 & 0 & 0 & -0.02 & 0.00429 & -0.00135 & 0.0443 & -0.00573 \\
-0.481 & -2.25 & 0.968 & 0 & -0.0251 & -0.00515 & 0.000256 & 0 & -0.251 & 0.0723 & -0.000526 & -0.00393 & 1.8 \\
2.29 & -20.8 & -3 & 0 & -0.721 & -0.135 & 0.00624 & 0 & -43.3 & 2.66 & -0.0438 & 0.00288 & 53 \\
0 & 0 & 1 & 0 & 0 & 0 & 0 & 0 & 0 & 0 & 0 & 0 & 0 \\
-0.000542 & 0.0115 & 0 & 0 & -0.561 & 0.0711 & -0.988 & 0.211 & 0 & 0.00624 & 0.215 & 0 & -0.0251 \\
-34.4 & -158 & -0.504 & 0 & -66 & -3.22 & 0.494 & 0 & 0.638 & 22 & 11.3 & 0.00735 & -797 \\
-3.76 & -21.8 & -0.0508 & 0 & 25.9 & -0.277 & -1.03 & 0 & 0.0209 & 1.84 & -28.7 & 0.0208 & -86.7 \\
0 & 0 & 0 & 0 & 0 & 1 & 0.0716 & 0 & 0 & 0 & 0 & 0 & 0
\end{array}\right] \tag{44}
$$

Acknowledgments

This research was funded by the National Natural Science Foundation of China (Grant Nos. 61273099 and 61304030) and the Fundamental Research Funds for the Central Universities (NJ20160026).

Notation

The following symbols are used in this paper:

$\boldsymbol{A}$ = state matrix;
a = aileron;
$\boldsymbol{B}$ = control matrix;
$\boldsymbol{C}$ = output matrix;
$\boldsymbol{d}$ = modeling error;
$\boldsymbol{F}(s)$ = filter matrix;
$\boldsymbol{f}_0$ = disturbance caused by damage;
$\boldsymbol{H}_d(s)$ = desired closed-loop transfer function;
$\boldsymbol{I}_n$ = identity matrix of size n;
$\boldsymbol{K}_1$ = feedback matrix;
$\boldsymbol{K}_2$ = feedforward matrix;
$\boldsymbol{K}_3$ = compensated control matrix;
$\boldsymbol{M}$ = control allocation matrix;
$\boldsymbol{O}$ = higher-order terms of Taylor series;
p = roll rate of aircraft (degrees/s);
q = pitch rate of aircraft (degrees/s);
r = yaw rate of aircraft (degrees/s);
$\mathcal{S}$ = model tensor;
$\boldsymbol{u}$ = input vector;
V = Lyapunov function;
$\boldsymbol{x}$ = state vector;
$\boldsymbol{y}$ = output vector;
α = angle of attack (degrees);
β = angle of slide (degrees);
$\boldsymbol{\alpha}$ = gain scheduling coefficient;
$\boldsymbol{\Gamma}$ = weight coefficient;
$\boldsymbol{\lambda}$ = damage parameter;
ζ = damping ratio;
θ = pitch angle (degrees);
ν = airspeed (m/s);
φ = roll angle (degrees);
ω_n = natural frequency (rad/s);
$*$ = vertex of convex set; and
$\#$ = grid index.

References

Airplanes, Boeing Commercial. 2016. *Statistical summary of commercial jet airplane accidents: Worldwide operations 1959–2015*. Seattle: Aviation Safety, Boeing Commercial Airplanes.

Åström, K. J., and B. Wittenmark. 1995. *Adaptive control: Addison-Wesley series in electrical engineering*. Reading, MA: Addison-Wesley.

Bacon, B. J., and I. M. Gregory. 2007. "General equations of motion for a damaged asymmetric aircraft." In *Proc., 2007 AIAA Atmospheric Flight Mechanics Conf. and Exhibit*, 1–13. Reston, VA: American Institute of Aeronautics and Astronautics.

Bailey, R. M., R. W. Hostetler, K. N. Barnes, C. M. Belcastro, and C. M. Belcastro. 2005. "Experimental validation: Subscale aircraft ground facilities and integrated test capability." In *Proc., AIAA Guidance Navigation, and Control Conf. and Exhibit*, 110. Reston, VA: American Institute of Aeronautics and Astronautics.

Bao, P., M. Yuan, H. Song, W. Guo, and J. Xue. 2011. "Aircraft wing structural damage localization research based on rbf neural network." In *Proc., 2011 IEEE 5th Int. Conf. on Cybernetics and Intelligent Systems*, 57–62. New York: IEEE.

Baranyi, P. 2016. "TP model transformation based control design structure." In *TP-model transformation-based-control design frameworks*, 25–29. New York: Springer.

Chowdhary, G., E. Johnson, R. Chandramohan, S. Kimbrell, J. Hur, and A. Calise. 2013. "Guidance and control of airplanes under actuator failures and severe structural damage." *J. Guidance Control Dyn.* 36 (4): 1093–1104. https://doi.org/10.2514/1.58028.

Di Sante, R. 2015. "Fibre optic sensors for structural health monitoring of aircraft composite structures: Recent advances and applications." *Sensors* 15 (8): 18666–18713. https://doi.org/10.3390/s150818666.

Giani, P., M. Tanelli, and M. Lovera. 2012. "Linear parameter-varying model identification with structure selection for autonomic web service systems." *IET Control Theory Appl.* 6 (12): 1889–1898. https://doi.org/10.1049/iet-cta.2011.0277.

Gilbert, E. G. 1969. "The decoupling of multivariable systems by state feedback." *SIAM J. Control* 7 (1): 50–63. https://doi.org/10.1137/0307004.

Guo, J., and G. Tao. 2012. "Discrete-time adaptive control of a nonlinear aircraft flight dynamic system (NASA GTM) with damage." In *Proc., 2012 IEEE 51st Annual Conf. on Decision and Control (CDC), IEEE Conf. on Decision and Control*, 1746–1751. New York: IEEE.

Guo, J., and G. Tao. 2015. "A discrete-time multivariable MRAC scheme applied to a nonlinear aircraft model with structural damage." *Automatica* 53: 43–52. https://doi.org/10.1016/j.automatica.2014.12.036.

Guo, J., G. Tao, and Y. Liu. 2011. "Multivariable adaptive control of NASA generic transport aircraft model with damage." *J. Guidance Control Dyn.* 34 (5): 1495–1506. https://doi.org/10.2514/1.53258.

Guo, J., G. Tao, and Y. Liu. 2014. "Adaptive actuator failure and structural damage compensation of NASA generic transport model." *J. Dyn. Syst. Meas. Contr.* 136 (3): 031009. https://doi.org/10.1115/1.4026162.

Ioannou, P. A., and J. Sun. 2012. *Robust adaptive control*. New York: Courier Corporation.

Jia, Q., W. Chen, Y. Zhang, and X. Chen. 2014. "Robust fault reconstruction via learning observers in linear parameter-varying systems subject to loss of actuator effectiveness." *IET Control Theory Appl.* 8 (1): 42–50. https://doi.org/10.1049/iet-cta.2013.0417.

Jordan, T., W. Langford, C. Belcastro, J. Foster, G. Shah, G. Howland, and R. Kidd. 2004. *Development of a dynamically scaled generic transport model testbed for flight research experiments*. Rep. No. 20040085988 Hampton, VA: NASA Langley Research Center.

Jung, B., Y. Kim, and C. Ha. 2009. "Fault tolerant flight control system design using a multiple model adaptive controller." *Proc. Inst. Mech. Eng. Part G: J. Aerosp. Eng.* 223 (1): 39–50. https://doi.org/10.1243/09544100JAERO360.

Khalil, H. K. 1996. *Nonlinear systems*. Upper Saddle River, NJ: Prentice-Hall.

Kim, K.-J., J. Ahn, S. Kim, J.-S. Choi, J. Suk, H. Lim, and G.-B. Hur. 2014. "Analysis of partial wing damage on flying-wing unmanned air vehicle." *Proc. Inst. Mech. Eng. Part G: J. Aerosp. Eng.* 228 (3): 355–374. https://doi.org/10.1177/0954410012472292.

Liu, Y., G. Tao, and S. M. Joshi. 2010. "Modeling and model reference adaptive control of aircraft with asymmetric damage." *J. Guidance Control Dyn.* 33 (5): 1500–1517. https://doi.org/10.2514/1.47996.

Lu, P., L. Van Eykeren, E. van Kampen, and Q. Chu. 2015. "Selective-reinitialization multiple-model adaptive estimation for fault detection and diagnosis." *J. Guidance Control Dyn.* 38 (8): 1409–1424. https://doi.org/10.2514/1.G000587.

Nguyen, N., K. Krishnakumar, J. Kaneshige, and P. Nespeca. 2008. "Flight dynamics and hybrid adaptive control of damaged aircraft." *J. Guidance Control Dyn.* 31 (3): 751–764. https://doi.org/10.2514/1.28142.

Ouellette, J. A. 2010. "Flight dynamics and maneuver loads on a commercial aircraft with discrete source damage." M.S. thesis, Dept. of Aerospace Engineering, Virginia Polytechnic Institute and State Univ.

Pei, Y., Z. Chen, Y. Wei, and T. Cheng. 2016. "Method for assessing combat survivability for aircraft with wing damage." *Proc. Inst. Mech. Eng. Part G: J. Aerosp. Eng.* 231 (5): 877–886. https://doi.org/10.1177/0954410016644629.

Qiu, L., S. Yuan, H. Mei, and F. Fang. 2016. "An improved Gaussian mixture model for damage propagation monitoring of an aircraft wing spar under changing structural boundary conditions." *Sensors* 16 (3): 291. https://doi.org/10.3390/s16030291.

Stepanyan, V., S. Campbell, and K. Krishnakumar. 2010. "Adaptive control of a damaged transport aircraft using m-MRAC." In *Proc., AIAA Guidance, Navigation, and Control Conf.*, 1–19. New York: American Institute of Aeronautics and Astronautics.

Sun, B., L. Yang, and J. Zhang. 2016. "Robust LPV control design based on HOSVD." [In Chinese.] *J. Beijing Univ. Aeronaut. Astronaut.* 42 (7): 1536–1542. https://doi.org/10.13700/j.bh.1001-5965.2015.0486.

Tao, G. 2014. "Multivariable adaptive control: A survey." *Automatica* 50 (11): 2737–2764. https://doi.org/10.1016/j.automatica.2014.10.015.

Vannieuwenhoven, N., R. Vandebril, and K. Meerbergen. 2012. "A new truncation strategy for the higher-order singular value decomposition." *SIAM J. Sci. Comput.* 34 (2): A1027–A1052. https://doi.org/10.1137/110836067.

Wang, X., Y. Miao, and S. Wang. 2016. "Active fault-tolerant control of large commercial aircraft with asymmetric damaged horizontal stabilizer." In *Proc., 2016 IEEE Int. Conf. on Aircraft Utility Systems (AUS)*, 780–785. New York: IEEE.

Xu, X., L. Yang, and J. Zhang. 2015. "MRAC control with prior model knowledge for asymmetric damaged aircraft." *Sci. World J.* 2015: 1–10.

Zhang, H., G. Zhang, and J. Wang. 2016. "Observer design for lpv systems with uncertain measurements on scheduling variables: Application to an electric ground vehicle." *IEEE/ASME Trans. Mechatron.* 21 (3): 1659–1670. https://doi.org/10.1109/TMECH.2016.2522759.